Time Delay Interferometry combinations as instrument noise monitors for LISA

Martina Muratore,[*] Daniele Vetrugno, and Stefano Vitale[†]

Dipartimento di Fisica, Universita di Trento and Trento Institute for
Fundamental Physics and Application / INFN, 38123 Povo, Trento, Italy

Olaf Hartwig

Max-Planck-Institut für Gravitationsphysik (Albert-Einstein-Institut),
Callinstraße 38, 30167 Hannover, Germany

(Dated: May 16, 2020)

Abstract

The LISA mission will likely be a signal dominated detector, such that one challenge is the separation of the different astrophysical sources, and to distinguish between them and the instrumental noise. One of the goals of LISA is to probe the early Universe by detecting stochastic GW backgrounds. As correlation with other detectors is not possible for LISA, discrimination of such a GW background from the instrumental noise requires a good estimate of the latter. To this purpose we have revisited Time Delay Interferometry (TDI) to look for new TDI signal combinations that fulfill the laser frequency noise suppression requirements. We illustrate that it is possible to do a linear combination of these TDI channels to find special null-combinations that suppress gravitational waves and mainly carry information about instrumental noise. We find that there exist many null-combinations that show different sensitivities to gravitational waves, some of which seem more suitable than the traditional T combination for estimating test-mass acceleration noise. In an idealised LISA configuration, they are all sensitive to a particular linear combination of the six test-masses acceleration, similar to a rigid rotation of the LISA triangle.

In the following article, we illustrate what are the noise properties that can be extracted by monitoring these interferometry signals and discuss the implication of these findings for the detection of stochastic GW backgrounds.

---

[*] contact: martina.muratore@unitn.it

[†] contact: stefano.vitale@unitn.it

1

1. INTRODUCTION

We have recently revisited the time-delay-interferometry (TDI) combinations that suppress laser noise in LISA [1], but we also found 24 new combinations of 14-links that fullfill the frequency noise suppression requirements that had been skipped previously [2, 3]. The total TDI combinations include 174 combinations of 16-links, 24 combinations of 14-links and 12 of 12 links for a total of 210 [4]. The LISA detector is expected to be signal dominated, thus to measure the instrumental noise we look for TDI combinations that have suppressed sensitivity to gravitational wave (GW) signals but still carry some information on the instrumental noise.

We find that a good proxy for such a property is for the combinations to be perfectly insensitive to GW when the arm lengths are equal and constant and the wave is propagating normally to such a perfect idealised LISA configuration. In this ideal condition, the signal out of any TDI combination becomes a linear combination of a finite set of single link signals with delays also chosen from a finite set. This allows to explore the space of all linear combinations of all possible TDI combinations, and to identify its null space, i.e. the set of all combinations that gives zero response to GW.

We find that the rank of such null space is just 7 and that the 7 fundamental combinations all give a, differently delayed, measurement of the same combination of TM accelerations. This combinations has a symmetry that resembles the rigid rotation of the constellation, and is different from that which enters in GW sensitive TDI combinations as, for instance, the second generation Michelson X.

The article is divided in five main sections. In the first section we use linear algebra to determine which are the TDI combinations that are insensitive to GW signals in case of a perfect orthogonal source considering a static LISA with equal arm-length. In the second section we use the method of single value decomposition to retrieve the instrumental noise of these combinations. In the third section, we give an estimate of the behaviour of these null-channels in case the LISA constellation undergoes small amplitude static distortions. Moreover, we compute the sensitivity both for a perfect LISA triangle and a non perfectly equilateral triangle, and we also validate our model of the test-mass (TM) acceleration noise with the outcome of numerical simulations performed using the python tools LISANode [5]

and PyTDI. Here, we show that some combinations deviate significantly from the simplified case when taking unequalities in the arms into account. For example, the traditional T null channel appears to have the same GW sensitivity as X in this more realistic scenario. The last section reports our conclusion and future perspective regarding the leverage of these null channels to calibrate the instrument during operations and we discuss the implication of these findings for the detection of stochastic GW backgrounds.

2. TDI COMBINATIONS WITH REDUCED SENSITIVITY TO GRAVITATIONAL WAVES

The full list of TDI combinations up to a length of 16 links has been revisited with respect to [1]. The lists of all 28 core combinations of 16 links, plus the 3 combinations of 12 links and the 3 of 14 links are shown in Tables I, II and III.

The combinations within this minimum set fall in a few simple categories, marked by: the number of emission/measurements event pairs, which ranges from 1 to 6, the number of arms involved, 2 or 3 and finally the number of inter-satellite links, 4 or 6, out of the six possible ones ($1 \rightarrow 2$, $2 \rightarrow 1$, $1 \rightarrow 3$, $3 \rightarrow 1$, $2 \rightarrow 3$, and $3 \rightarrow 2$) that are involved in the sequence. As an example, the standard TDI X, that in our notation is C_1^{16}, shows up on the first line of Table I. It only involves 2 arms, 4 inter-SC links and 1 measurement event.

Note that these core combinations can be used to generate all 210 TDI channels by applying the appropriate symmetries and index permutations. The TDIs C_3^{12}, C_3^{14}, C_{26}^{16}, C_{27}^{16} have the properties of being fully symmetric in the idealistic scenario of equal and constant arm-length. In fact, they represent second generation versions of the first generation fully symmetric Sagnac combination known from the literature [6]. Note, however, that they are different from the second generation versions reported there.

We will mostly focus on the fully symmetric combination with the minimum number of links that is the C_3^{12} to which we simply refer by ζ in the following.

See Supplemental Material at [URL] for the full set of TDI combinations.

Number of combination	Combination	Number of measurements	Number of arms	Number of inter-SC-links	Number of combination	Combination	Number of measurements	Number of arms	Number of inter-SC-links
$\mathcal{C}_1^{16}$	1→2→1→3→1→3→1→2←1←3←1←2←1←2←1←3←1	1	2	4	$\mathcal{C}_{15}^{16}$	1→2→1→3→2←1←2←3→1→2→1←3←2←1←2→3←1	3	3	6
$\mathcal{C}_2^{16}$	1→2→1→3→2→3→1→2←1←3←2←1←2←1←2←3←1	1	3	6	$\mathcal{C}_{16}^{16}$	1→2→1→3←2←1←2→3←2←1←2←3→1→2→1←3←1	3	3	6
$\mathcal{C}_3^{16}$	1→2→3→1→2→1→3→2←1←3←2←1←2←1←2←3←1	1	3	6	$\mathcal{C}_{17}^{16}$	1→2→1→3→2←1←3←2←1←3→1→2←3←1←2→3←1	3	3	6
$\mathcal{C}_4^{16}$	1→2→2→1←3←1←2←1→3→1→3→1←2←1←3←1	2	2	4	$\mathcal{C}_{18}^{16}$	1→2→1←3←2←1←3→2→1←3←1→2←3→1←2←3←1	3	3	6
$\mathcal{C}_5^{16}$	1→2→1→3→1→2←1←3←1←2←1→3←1←2←1←3←1	2	2	4	$\mathcal{C}_{19}^{16}$	1→2→3→2→3→2←1←3←2←1←3←2←3→1←2←3←1	3	3	6
$\mathcal{C}_6^{16}$	1→2→1→3→2→1→2←3←1←2←1→3→2←1←2←3←1	2	3	4	$\mathcal{C}_{20}^{16}$	1→2→3→2→3→2←1←3←2←3←1←2←1←3←2←3←1	3	3	6
$\mathcal{C}_7^{16}$	1→2→3→1→2→3←1←3←2←1→3→1→3←2←1←3←1	2	3	4	$\mathcal{C}_{21}^{16}$	1→2→1←2←3←1←2←1→3←2←1→3←2←1←2→3←1	4	3	4
$\mathcal{C}_8^{16}$	1→2→3→1→3→1→2→3←1←3←2←1←3←2←1←3←1	2	3	4	$\mathcal{C}_{22}^{16}$	1→2→1←3←2←1←2←3←1←2←3←1→2→1←3←1	4	3	4
$\mathcal{C}_9^{16}$	1→2→1←2←3←2←1←2→3→1→3→2←1←2←3←1	2	3	6	$\mathcal{C}_{23}^{16}$	1→2→1←3→2←1←2→3→1←3←2←1←2→3←1	4	3	6
$\mathcal{C}_{10}^{16}$	1→2→1→3→1→2←1←3←2←1←2→3→2←1←2←3←1	2	3	6	$\mathcal{C}_{24}^{16}$	1→2→3←1←2←1←3←2←1→3→2←1←3←1←2←3←1	4	3	6
$\mathcal{C}_{11}^{16}$	1→2→3→1→2→3→2←1←3←2←1←3←2←1←2←3←1	2	3	6	$\mathcal{C}_{25}^{16}$	1→2→3→2←1←3←2←3←1←2←3→2←1←3←2←3←1	4	3	6
$\mathcal{C}_{12}^{16}$	1→2→3→1→3→2→1←3←1←2←3→1←3←2←1←3←1	2	3	6	$\mathcal{C}_{26}^{16}$	1→2→1←2←3→2←1←3←2←1←2←3←1←2→3←1	5	3	6
$\mathcal{C}_{13}^{16}$	1→2→1→2←1←3←2←1→3←2←1←2→3←2←1←3←1	3	3	6	$\mathcal{C}_{27}^{16}$	1→2→1←3→2←1←2→3←2←1←3←1←2←3←1←2→3←1	5	3	6
$\mathcal{C}_{14}^{16}$	1→2→1→3→1→2→1←3→2←1←2←3←2←1←2→3←1	3	3	6	$\mathcal{C}_{28}^{16}$	1→2→1←3←2→1←3←2←1←3→1←2→3←2←1←2→3←1	6	3	6

TABLE I. 16-links TDI combinations that suppress laser noise. C_i^{16} is the sequence number. Each combinations is represented with numbers and arrows: numbers within each sequence indicate the satellite on which each event takes place. First and last event coincide. Arrows indicate the direction of the link connecting adjoining events. Events at the start of two arrows represent simultaneous emission of two beams. Events at the end of two arrows represent measurements. Events between arrows going in the same direction indicate that the SC transponders/relays the beam to the next that follows. The first is always an emission event. The last three columns indicates the number of measurements events, the number of arms and number of inter-SC links involved in the sequence, respectively.

Number of combination	Combination	Number of measurements	Number of arms	Number of inter-SC-links	Number of combination	Combination	Number of measurements	Number of arms	Number of inter-SC-links
$\mathcal{C}_1^{14}$	1→2→1→3→2→1←3←2←1←2→3→1←2←3←1	2	3	6	$\mathcal{C}_3^{14}$	1→2→1→3←2→1←3→2←1←2←3→1←2→3←1	5	3	6
$\mathcal{C}_2^{14}$	1→2→1→3←2←1←3→2←1←2←3→1→2→3←1	3	3	6					

TABLE II. 14-link TDI combinations that suppress laser noise. Definitions are the same as those for TABLE I

Number of combination	Combination	Number of measurements	Number of arms	Number of inter-SC-links	Number of combination	Combination	Number of measurements	Number of arms	Number of inter-SC-links
$\mathcal{C}_1^{12}$	1→2→3→1→3→2←1←3←2←1←2←3←1	1	3	6	$\mathcal{C}_3^{12}$	1→2→1←3←2←1→3←2←3→1←2→3←1	5	3	6
$\mathcal{C}_2^{12}$	1→2→3→2→1←3←2←1←1→3←1←2←3←1	2	3	6					

TABLE III. 12-link TDI combinations that suppress laser noise. Definitions are the same as those for TABLE I.

In order to look for TDI combinations that are insensitive to GW signals, we calculate their sensitivity to GW coming orthogonal to LISA, in the idealised equilateral, constant arm-length configuration (see Fig. 1). Indeed, to do a quick search one can focus on frequencies for which the maximum delay among the various link signals, 8τ, has negligible
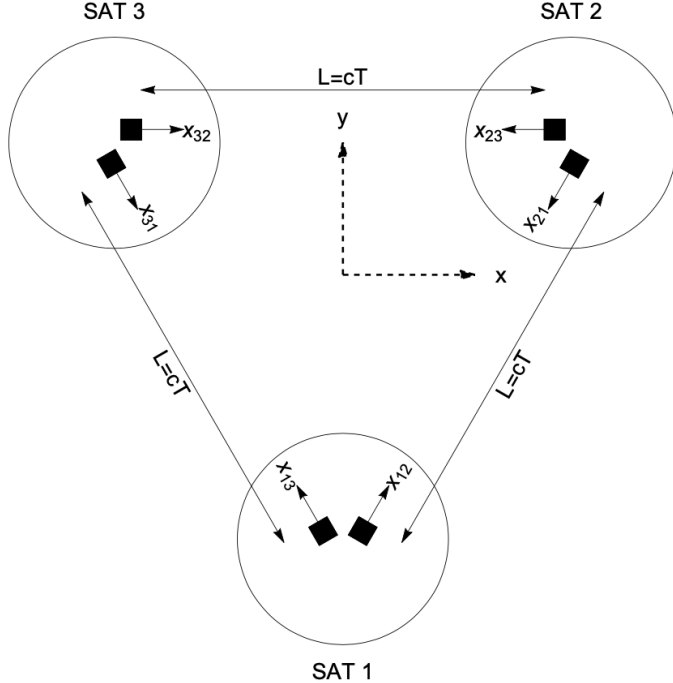
FIG. 1. Schematics of the idealised LISA geometry. Three satellites (indicated as SAT), shown as circles, include two test-masses, shown as black squares, each. The satellites are at the vertexes of an equilateral triangle in the x-y plane, with orientation relative to the axes as shown in the picture. The figure also shows the numbering convention for the satellites, and the orientation chosen as positive, for the displacement $x_{j,i}$ of the TM in satellite j at the end of the link from satellite i.

impact, that is, for which $2\pi f \times 8\tau \ll 1$. For $c\tau = L = 2.5\,\mathrm{Gm}$ this suggests frequencies below $20\,\mathrm{mHz}$.

A TDI combinations that gives zero signal in this simplified case is expected to suppress the signal in realistic situation. An example of these TDI combinations that we are looking for is the combination known as T, given for example in [7].

Regarding the instrumental noises, we consider only the effect of acceleration noise, as this is to be the dominant noise source of the LISA instrument below a few mHz [8].

We can summarize the LISA measurements principle by considering how the GW signal enters into a single interspacecraft link. One of the satellites, called the emitter, sends a beam to a second one, the receiver, which measures the frequency or phase of the received beam. GWs are detected as a modulation of the frequency or phase of the received beam.

In units of frequency, the response of a link to the GW signal is given as [9]:

$$\Delta\nu_h = \frac{\nu_0}{2(1 - \hat{k}_{GW} \cdot \hat{n})} \left(\mathbf{h}_{ij}\left(t_e - \frac{\hat{k}_{GW} \cdot \vec{r}_e}{c}\right) - \mathbf{h}_{ij}\left(t_r - \frac{\hat{k}_{GW} \cdot \vec{r}_r}{c}\right) \right) n^i n^j, \qquad (1)$$

where $\hat{k}_{GW}$ is the versor that describes the direction of propagation of the gravitational wave from the source to the detector, ν_0 is the nominal laser frequency, $\hat{n}$ stands for the LISA link versor, t_e and t_r are the emission and reception time of the beam, respectively, and $\vec{r}_e$ and $\vec{r}_r$ are the satellites position vectors. All these quantities are expressed in the Solar System reference frame [10].

Let us introduce some nomenclature that will be useful in the next paragraph. The symbol $x_{j,i}$, as illustrated in Fig. 1, represents the time-series of the relative displacement of the TM located inside satellite j and at the end of the link starting from satellite i. The relative displacement of the TM is considered along the direction of the link and it is relative to the local inertial frame. Within the assumptions given before and accordingly to the center of mass (COM) reference frame $\hat{x} - \hat{y}$ in Fig. 1, we can compute the interferometric signals in the six LISA links that can be described in frequency as illustrated in TABLE IV.

To do the calculation, we consider the approximation that all delays are constant and equal to τ. As we will see in section 4, this assumption holds well for some combinations, like the classic Michelson X, while others deviate significantly in the more realistic case of unequal armlengths. Still, it is a good working assumption to descibe the single link signals, especially in the low-frequency regime.

These assumptions will allow us to use linear algebra to find all combinations of the 210 TDI combinations, reported in the supplement material, which are null to GW and can be used to measure the instrumental noise.

Considering the low frequencies regime, in the approximation of constant and equal delays, the expression for the GW signal for a general TDI_k combination can be computed as [11]:

$$h[TDI_k](t) = \sum_{j=0}^{8}(a_{k,j}^{+}h_{+}(t - j\tau) + a_{k,j}^{\times}h_{\times}(t - j\tau)) \equiv \sum_{j=1}^{18} a_{k,j}h_j(t). \qquad (2)$$

Here, $a_{k,j}^{+}$ and $a_{k,j}^{\times}$ are the coefficients of h_{+} and $h_{\times}$, computed using TABLE IV for all the

6

Link	$\Delta\nu$
$2 \to 1$	$\frac{\nu_0(t)}{c}\left(\dot{x}_{1,2}(t) + \dot{x}_{2,1}(t-\tau)\right) - \frac{\nu_0(t)}{4}(h_+(t) - h_+(t-\tau)) + \frac{\nu_0(t)\sqrt{3}}{4}(h_\times(t) - h_\times(t-\tau))$
$1 \to 2$	$\frac{\nu_0(t)}{c}\left(\dot{x}_{1,2}(t-\tau) + \dot{x}_{2,1}(t)\right) - \frac{\nu_0(t)}{4}(h_+(t) - h_+(t-\tau)) + \frac{\nu_0(t)\sqrt{3}}{4}(h_\times(t) - h_\times(t-\tau))$
$3 \to 1$	$\frac{\nu_0(t)}{c}\left(\dot{x}_{1,3}(t) + \dot{x}_{3,1}(t-\tau)\right) - \frac{\nu_0(t)}{4}(h_+(t) - h_+(t-\tau)) - \frac{\nu_0(t)\sqrt{3}}{4}(h_\times(t) - h_\times(t-\tau))$
$1 \to 3$	$\frac{\nu_0(t)}{c}\left(\dot{x}_{1,3}(t-\tau) + \dot{x}_{3,1}(t)\right) - \frac{\nu_0(t)}{4}(h_+(t) - h_+(t-\tau)) - \frac{\nu_0(t)\sqrt{3}}{4}(h_\times(t) - h_\times(t-\tau))$
$3 \to 2$	$\frac{\nu_0(t)}{c}\left(\dot{x}_{3,2}(t-\tau) + \dot{x}_{2,3}(t)\right) + \frac{\nu_0(t)}{2}(h_+(t) - h_+(t-\tau))$
$2 \to 3$	$\frac{\nu_0(t)}{c}\left(\dot{x}_{3,2}(t) + \dot{x}_{2,3}(t-\tau))\right) + \frac{\nu_0(t)}{2}(h_+(t) - h_+(t-\tau))$

TABLE IV. Table of the six single LISA links expressed in units of frequency for a GW wave propagating normal to the LISA plane. The symbol $x_{j,i}$ is the small signal displacement of the TM located inside satellite j, and at the end of the link starting from satellite i, and $\dot{x}_{j,i}$ is its derivative. h_+ and $h_\times$ are the plus and cross polarization of the GW signal and their respective coefficients follow from the projection of the GW along the LISA link.

210 combinations. Since we have 9 coefficients for each of the $+$ and $\times$ polarizations, we count a total of 18 $a_{k,j}$ coefficients for each combination.

We also calculate the signal due to acceleration of the TMs which has the form:

$$g[TDI_k](t) = \sum_{j=0}^{8} \sum_{i\neq n=1}^{3} b_{kinj} g_{i,n}(t - j\tau) \equiv \sum_{j=1}^{54} \sum_{i\neq n=1}^{3} \beta_{kj} g_{j,n}(t), \qquad (3)$$

where b_{kinj} are the coefficients of the six TMs acceleration terms $g_{i,n} = \ddot{x}_{i,n}$ computed for each time $t-j\tau$. The equation has been computed considering that each TM has two indices: the first one stands for satellite i the TM is located in, while the second one, n, stands for which satellites the TM faces. Both indices i and n can go from 1 to 3, with the restriction that $i \neq n$. Note that $g_{i,n} \neq g_{n,i}$, as these terms describe different test masses. Similar to Eq. (2), there are nine measuring time, such that we have a total of 54 coefficients β_{kj} for the six test masses.

We can now look for linear combinations of the combinations that form Eq. (2), which we call $\psi_l(t)$, that are insensitive to GWs:

$$\psi_l(t) = \sum_{k=1}^{N} c_{lk} h[TDI_k](t) = 0, \qquad (4)$$

where N is the total number of laser noise suppressing TDI combinations. There are multiple

solutions for $\psi_l(t)$, which are distinguished by the label l.

We can insert Eq. (2) into Eq. (4) and consider each h_j to be independent to conclude that $\psi_l(t)$ is zero under the condition that

$$\sum_{k=1}^{N} c_{lk}\alpha_{k,j} = 0. \tag{5}$$

Thus, any row l of the null space of the matrix $\alpha_{k,j}^T$ contains the coefficients c_{lk} of one possible linear combination of the 210 TDIs null to GW.

We find that the null space matrix has 200 rows, i.e. there are 200 possible combinations that cancel the GW signal. This means that there are 200 ways of combining our 210 laser noise cancelling TDI combinations to find new combinations that give no GW signal.

Once the null space c_{lk} has been found, we can calculate the TM acceleration signals $g[\psi_l](t)$ for each combinations l null to GW as following:

$$g[\psi_l](t) = \sum_{k=1}^{N} c_{lk} \sum_{j=1}^{54} \beta_{kj} g_j(t). \tag{6}$$

It turns out that for some value of l these combinations are also null to acceleration noise, that is, $\sum_{k=1}^{N} c_{lk} \sum_{j=1}^{54} \beta_{kj} = 0$. We find a total of 24 out of the 200 combination that in the equal arms configuration, give no output. This means that at least in the approximation of equal arms, these combinations do not measure anything, and we discard them for the further analysis. We will investigate the underlying reason for this effect in a follow up work [12].

We will continue our analysis using only the remaining 176 combinations, see Supplemental Material at [URL] for the listed combinations in TABLE IV, and to which we will refer in the following as the null-channels [13]. We remark that combination number 176 of that list is the T combination that is given as the sum of the three Michelson combinations. Notice also that, out of these 176 null channels, there are 21 which are single TDI combinations that already suppress the GW signal on their own.

Furthermore, it is found out that the rank of the matrix of coefficient δ_{ij},

$$\delta_{ij} = \sum_{k=1}^{N} c_{ik} \sum_{j=1}^{54} \beta_{kj}, \tag{7}$$

is 7. Thus, most of the null-channels which have a non zero acceleration signal contain redundant information. In the next section we follow the method of the single value decomposition to decompose the matrix and see if we are able to retrieve the single TM acceleration noises.

3.   SINGLE VALUE DECOMPOSITION TO RETRIEVE THE ACCELERATION NOISE SIGNALS

As we found out that the rank of the null space is 7, we will continue our search considering a reduced set of combinations which will include just the two cyclic SC permutation symmetries (we neglect the other symmetries). This new set allows to have an isotropic representation of the TDI space [14] while improving the machine computation time.

This reduced set contains a total of 102 combinations, and yields 92 null channels free of GW signals. As we saw in the previous section, there are six test masses and nine measuring times, such that the acceleration signals enter with 54 distinct coefficients. To retrieve which of the combinations are independent, we can do the singular value decomposition of the 92×54 matrix as expained in Appendix A. The results is a combination of the acceleration coefficients β_{kj} which we call $g[\psi_m](t)$. These combinations of combinations are represented by:

$$g[\psi_m](t) = \sum_{i=1}^{N_{\text{null}}} U_{mi}^{-1} \sum_{k=1}^{N_{TDI}} c_{ik} \sum_{j=1}^{54} \beta_{kj} g_j(t), \tag{8}$$

where $N_{\text{null}} = 92$ is the number of null channels, $N_{TDI} = 102$ the total number of TDI combinations we considered and c_{lk} are the coefficients that belong to the null-space of the matrix, while U_{mi} is a 92×92 matrix. We empirically found that the 54 $g_j(t)$ elements, after

this operation, appear only in the following form:

$$g[\psi_m](t) = \sum_{n=0}^{8} \epsilon_{mn} G_n(t). \tag{9}$$

The index m goes from 1 to 7 as we have 7 independent signals. The 9 combinations $G_n(t)$ that appear are combinations of the following quantities for any value of the coefficient n:

$$\begin{aligned} G_n(t) =& g_{1,2}(t - n\tau) - g_{2,1}(t - n\tau) + g_{3,1}(t - n\tau) \\ &- g_{1,3}(t - n\tau) + g_{2,3}(t - n\tau) - g_{3,2}(t - n\tau). \end{aligned} \tag{10}$$

It is then useful to compare these signals $G_n(t)$ with that entering the X combination:

$$G_{X_n}(t) = g_{1,2}(t - n\tau) + g_{2,1}(t - n\tau) - g_{1,3}(t - n\tau) - g_{3,1}(t - n\tau). \tag{11}$$

The symmetry of the Eq. (10) it's worth investigating. If we simplify the problem and reduce the six LISA test-masses to three test-masses, that coincide with the vertex of a triangle, one can decompose the acceleration $g_{j,i}(t)$ into linear combinations of the modes of an equilateral spring-mass triangle, and readily calculate that only rotation has a non zero projection onto $G_n(t)$ as visible in Fig. 2. Conversely, the Michelson combination X shows to be sensitive to a different mode of the triangle that is displayed in Fig. (3). Notice that this is the *a-mode* and it is orthonormal to the rotation mode. In other words, considering a perfect drag-free attitude control system and that each spacecraft is rigidity connected to the test-masses, if we rotate the constellation around the LISA COM, the type of signal we see, in first approximation, can be considered as representing the rigid rotation of the constellation. This is the only thing we can measure in this set up, which implies that if we loose the laser link in one arm we would also loose our ability to construct a null channel.

The corresponding coefficients' matrix ϵ_{mn} (7×9) for each time value (n goes from 0 to 9) of $G_n(t)$ is reported in Table V.

However, it is possible to further simplify the problem by taking the difference of G_0, G_1, G_2, G_3, G_4, G_5, G_6, G_7 and G_8 i.e. the differences of the acceleration signals. We are
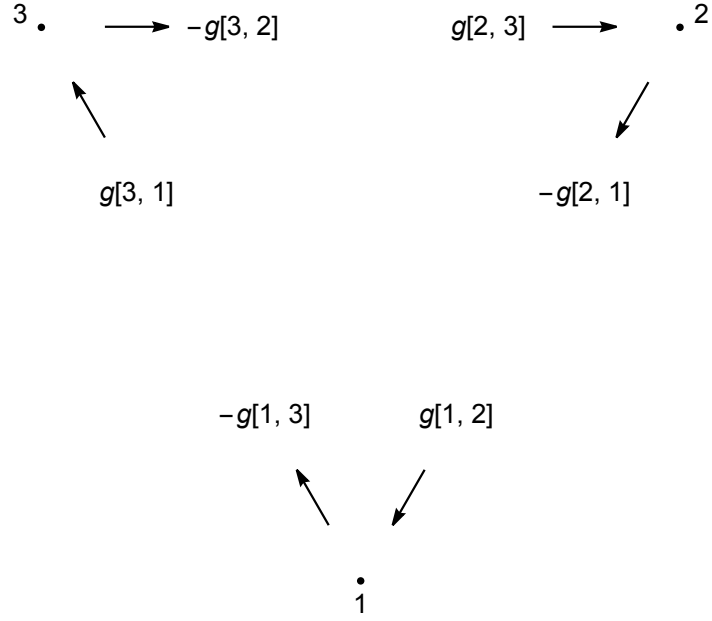
FIG. 2. Acceleration signal for the null combinations projected along the LISA arms. All null combinations in the case of a simplified constant equal arm-lengths configurations behave as an ideal Sagnac interferometer.
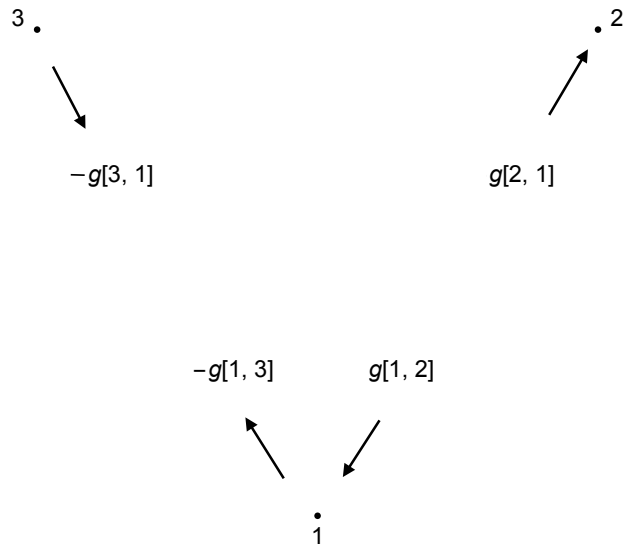

FIG. 3. Acceleration signal for the TDI X projected along the LISA arms. The TDI X in the case of a simplified constant equal arm-lengths configurations is sensitive to the a-mode of a triangle.

then able to further reduce the matrix ϵ_{mn} from a 7×9 matrix to a 7×7 matrix, using the

	G_0	G_1	G_2	G_3	G_4	G_5	G_6	G_7	G_8
ψ_1	$\frac{137}{12}$	$-\frac{464}{25}$	$-\frac{142}{23}$	$\frac{314}{19}$	$\frac{140}{33}$	$-\frac{285}{32}$	$\frac{317}{222}$	$-\frac{53}{508}$	$\frac{110}{833}$
ψ_2	$-\frac{105}{37}$	$\frac{96}{25}$	$-\frac{34}{9}$	$\frac{157}{17}$	$-\frac{356}{37}$	$\frac{155}{43}$	$\frac{39}{100}$	$-\frac{119}{149}$	$\frac{5}{144}$
ψ_3	$\frac{74}{75}$	$-\frac{49}{12}$	$\frac{14}{3}$	$-\frac{7}{9}$	-3	$\frac{11}{3}$	$-\frac{3}{10}$	$-\frac{8}{5}$	$\frac{94}{203}$
ψ_4	$-\frac{89}{39}$	$\frac{32}{153}$	$\frac{298}{77}$	$\frac{75}{61}$	$-\frac{124}{111}$	$-\frac{134}{33}$	$\frac{69}{44}$	$\frac{79}{84}$	$-\frac{109}{305}$
ψ_5	$-\frac{199}{140}$	$\frac{55}{227}$	$\frac{94}{147}$	$\frac{127}{109}$	$\frac{49}{37}$	$\frac{48}{71}$	$-\frac{41}{19}$	$\frac{59}{149}$	$\frac{47}{124}$
ψ_6	$-\frac{55}{107}$	$\frac{21}{86}$	$\frac{3}{31}$	$\frac{125}{368}$	$\frac{135}{212}$	$-\frac{73}{328}$	$\frac{116}{567}$	$-\frac{223}{103}$	$\frac{109}{79}$
ψ_7	$-\frac{47}{124}$	$-\frac{57}{370}$	$\frac{16}{279}$	$\frac{34}{299}$	$\frac{59}{156}$	$\frac{82}{217}$	$\frac{287}{383}$	$-\frac{7}{27}$	$-\frac{227}{295}$

TABLE V. Table of the ϵ_{mn} coefficients for the 7 independent combinations in case of LISA with constant and equal arm-length.

	ΔG_0	ΔG_1	ΔG_2	ΔG_3	ΔG_4	ΔG_5	ΔG_6	ΔG_7	ΔG_8
ψ_1	0	0	$\frac{8}{3}$	$\frac{70}{3}$	$-\frac{40}{3}$	$-\frac{34}{7}$	$\frac{22}{5}$	$-\frac{20}{21}$	$\frac{7}{53}$
ψ_2	0	0	$-\frac{19}{2}$	$\frac{46}{3}$	$-\frac{113}{7}$	$\frac{51}{4}$	$-\frac{37}{6}$	$\frac{14}{13}$	$-\frac{5}{144}$
ψ_3	0	0	-4	12	$-\frac{25}{2}$	$\frac{17}{3}$	$\frac{3}{2}$	$-\frac{19}{9}$	$\frac{19}{41}$
ψ_4	0	0	$-\frac{13}{2}$	$-\frac{1}{2}$	10	$-\frac{56}{11}$	$-\frac{13}{7}$	$\frac{23}{12}$	$-\frac{5}{14}$
ψ_5	0	0	$-\frac{79}{5}$	$\frac{112}{3}$	$-\frac{121}{3}$	$\frac{126}{5}$	-10	$\frac{29}{11}$	$-\frac{11}{29}$
ψ_6	0	0	-1	$-\frac{25}{4}$	$\frac{47}{2}$	$-\frac{131}{4}$	$\frac{71}{3}$	$-\frac{71}{8}$	$\frac{29}{21}$
ψ_7	0	0	$-\frac{47}{5}$	$\frac{127}{4}$	$-\frac{99}{2}$	$\frac{131}{3}$	$-\frac{113}{5}$	$\frac{77}{12}$	$-\frac{10}{13}$

TABLE VI. Table of the ϵ_{mn} coefficients for the 7 independent combinations in case of LISA with constant and equal arm-length via the new difference variable ΔG_n. Note that the relation can be inverted to give the ΔG_k for $k \geq 2$

backward finite differences of $G_n(t)$ [15] i.e.,

$$\Delta G_n = (-1)^k \sum_{k=0}^{8} \binom{n}{k} G_k.$$

Thus, we can reduce the set of 9 signals from G_0 to G_8 by using these new difference variables and obtain an invertible matrix made out of the ΔG_n. Notice that switching to ΔG_n causes the term ΔG_0 and ΔG_1 to disappear. So, in this way, if we use the analogy with a backward finite differences of $G_n(t)$ the minimum quantity we can measure is a second

derivative of the ΔG and the relation can be inverted to give the ΔG_k for $k \geq 2$.

However, since the rank of the previously obtained null space is 7, we do not really need to start our analysis using such a large set of TDI combinations, and we can try to reduce the set of 102 combinations we are using even further. Therefore, instead of building the null-channels by linearly combining the three copies of the original core obtained by the two cyclic permutations of spacecraft indices, we applied the same criterion that is currently used to build the combination T for all core TDI combinations. That is: we produce a new set of combinations $\tilde{C}_k$ by averaging the signals over the combinations obtained by applying the two cyclic permutations of the satellites to the 34 core combinations. Note that an advantage of this approach is that we directly obtain a new set of combinations which are null to GWs in the case of a perfect equilateral LISA, so we do not have to look for the null space [16].

Furthermore, we consider here only 31 combinations out of the 34 since we exclude three core combinations that we found to not bring any informations when considering equal arms that are C_4^{16}, C_{24}^{16} and C_{28}^{16}. Indeed as we will show in detail in a follow up work [12], these combinations in case of constant and equal arm-length give no output, while they strongly suppress both noise and GW signals in the realistic case of unequal, time-varying arms.

It turns out that there are many possible independent combinations we can form by applying the two cyclic permutations of the satellites out of the combinations listed in Tables I, II and III. From empirical studies we found that the ones that have the minimum number of links involved yield simpler expressions for estimating the acceleration noise, while containing the same information as any other set. These TDIs channels are $\tilde{C}_1^{16}, \tilde{C}_2^{16}, \tilde{C}_1^{14}, \tilde{C}_3^{14}, \tilde{C}_1^{12}, \tilde{C}_2^{12}, \tilde{C}_3^{12}$. In Table VII we compute the acceleration signals for this set.

The matrix of coefficients from Table VII can be inverted to give the ΔG_k for $k \geq 2$:

	ΔG_0	ΔG_1	ΔG_2	ΔG_3	ΔG_4	ΔG_5	ΔG_6	ΔG_7	ΔG_8
$\tilde{\mathcal{C}}_1^{16}$	0	0	0	0	$-\frac{8}{3}$	$\frac{16}{3}$	$-\frac{14}{3}$	2	$-\frac{1}{3}$
$\tilde{\mathcal{C}}_2^{16}$	0	0	-2	6	$-\frac{32}{3}$	$\frac{34}{3}$	-7	$\frac{7}{3}$	$-\frac{1}{3}$
$\tilde{\mathcal{C}}_1^{14}$	0	0	-2	3	$-\frac{5}{3}$	$\frac{1}{3}$	0	0	0
$\tilde{\mathcal{C}}_3^{14}$	0	0	-2	1	0	0	0	0	0
$\tilde{\mathcal{C}}_1^{12}$	0	0	-3	6	-5	2	$-\frac{1}{3}$	0	0
$\tilde{\mathcal{C}}_2^{12}$	0	0	-1	1	$-\frac{1}{3}$	0	0	0	0
$\tilde{\mathcal{C}}_3^{12}$	0	0	-1	0	0	0	0	0	0

TABLE VII. Matrix of coefficients of the acceleration signal for the set $\tilde{\mathcal{C}}_1^{16}, \tilde{\mathcal{C}}_2^{16}, \tilde{\mathcal{C}}_1^{14}, \tilde{\mathcal{C}}_3^{14}, \tilde{\mathcal{C}}_1^{12}, \tilde{\mathcal{C}}_2^{12}, \tilde{\mathcal{C}}_3^{12}$. The matrix can be inverted to give the ΔG_k for $k \geq 2$

$$\Delta G_2 = -\tilde{\mathcal{C}}_3^{12} \tag{12a}$$

$$\Delta G_3 = \tilde{\mathcal{C}}_3^{14} - 2\tilde{\mathcal{C}}_3^{12} \tag{12b}$$

$$\Delta G_4 = -3\left(\tilde{\mathcal{C}}_2^{12} + \tilde{\mathcal{C}}_3^{12} - \tilde{\mathcal{C}}_3^{14}\right) \tag{12c}$$

$$\Delta G_5 = 3\left(\tilde{\mathcal{C}}_1^{14} - 5\tilde{\mathcal{C}}_2^{12} - \tilde{\mathcal{C}}_3^{12} + 2\tilde{\mathcal{C}}_3^{14}\right) \tag{12d}$$

$$\Delta G_6 = -3\left(\tilde{\mathcal{C}}_1^{12} - 6\tilde{\mathcal{C}}_1^{14} + 15\tilde{\mathcal{C}}_2^{12} - 3\tilde{\mathcal{C}}_3^{14}\right) \tag{12e}$$

$$\Delta G_7 = -3\left(7\tilde{\mathcal{C}}_1^{12} - 24\tilde{\mathcal{C}}_1^{14} + \tilde{\mathcal{C}}_1^{16} + 39\tilde{\mathcal{C}}_2^{12} - \tilde{\mathcal{C}}_2^{16} - 4\tilde{\mathcal{C}}_3^{12} - 3\tilde{\mathcal{C}}_3^{14}\right) \tag{12f}$$

$$\Delta G_8 = -3\left(28\tilde{\mathcal{C}}_1^{12} - 76\tilde{\mathcal{C}}_1^{14} + 7\tilde{\mathcal{C}}_1^{16} + 96\tilde{\mathcal{C}}_2^{12} - 6\tilde{\mathcal{C}}_2^{16} - 16\tilde{\mathcal{C}}_3^{12}\right). \tag{12g}$$

Note that ΔG_2 is directly given as $-\tilde{\mathcal{C}}_3^{12}$, which turns out to be directly proportional to $\mathcal{C}_3^{12}$ (i.e. ζ), at least within our approximation. See [2] for more information. Moreover, ΔG_3 up to ΔG_6 can be estimated using just 12-link and 14-link combinations.

Therefore, since all ΔG_i are finite difference of the same signal, we show that every combination of TDI combinations you can use, up to 16 links long, give at most the same info as ζ. We can measure just the second discrete difference of a TM constellation rotation and other TDI combinations just measure higher order derivatives of the same signal.

In the next paragraph to validate the beforehand conclusion we translate this to a more
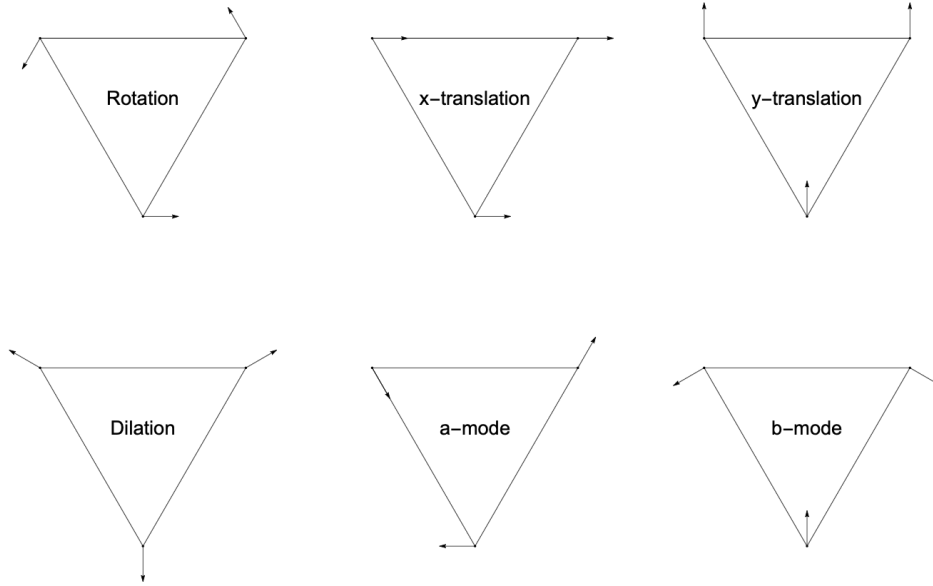
FIG. 4. Normal modes of an equilateral spring-mass triangle. Figure adapted form ref. [17].

realistic LISA model and assess the sensitivity for the null-channels ζ and T.

4. COMPUTATION OF THE EFFECTIVE H NOISE FOR A PERFECT LISA TRIANGLE AND A NON PERFECTLY EQUILATERAL TRIANGLE

Let us now relax the hypothesis of a perfectly equilateral LISA and compute the TM acceleration noise considering constant but not equal arm-lengths.

Since LISA is a constellation of satellites that form ideally an equilateral triangle, we decided to approach the problem of the inequality of the arm-lengths by assuming that LISA undergoes small amplitude static distortions along any of the triangle normal modes that are illustrated in Fig. 4.

We can then study the impact of the distortion modes following [17], and calculate which one causes an effective distortion with respect to the nominal LISA. To linear terms in the distortion, only the *a-mode*, *b-mode* and *d-mode* (Dilation) cause a change in the length of the arms. The dilatation mode shows to distort LISA equally in all the directions, such that it does not modify the assumption of equal arms. The *a-mode* and *b-mode*, however, cause a differential change between the arms, while leaving the overall perimeter of the triangle at its nominal value.

We therefore just consider the *a-mode* (δ_a) and *b-mode* (δ_b) and assume that all other modes have zero amplitude. Then, we can express the three LISA arms, to linear terms in the distortion, as:

$$L_{12} = c\tau \left(1 + \frac{1}{2} \left(\sqrt{3}\delta_a - \delta_b \right) \right)$$

$$L_{23} = c\tau \left(1 + \delta_b \right) \tag{13}$$

$$L_{31} = c\tau \left(1 - \frac{1}{2} \left(\sqrt{3}\delta_a + \delta_b \right) \right).$$

We define the root-mean square (RMS) deviation δ_r of the arm-length as:

$$\delta_r = \sqrt{\frac{\delta_a^2 + \delta_b^2}{2}}. \tag{14}$$

We then consider the leading order terms in the distortion for LISA with unequal but constant arm-length, to calculate in the frequency domain the response to a GW coming orthogonal with respect to LISA plane. We can do the same with the acceleration noise and expand both the acceleration signal and the GW signal as a function of frequency and take only the leading term at low frequency. In this process, we assume that all $g_{i,j}(\omega)$ have the same PSD $S_g(\omega)$, and calculate the effective h noise using the transfer function for $h_{rms} = \sqrt{h_+^2 + h_\times^2}$, as we will explain in the following. We refer to effective h noise as the level of the TM acceleration noise we would be able to detect in the presence of a GW background [18].

We can compute the effective h noise by considering that the output of a TDI$_j$, given a stochastic GW background, is a stochastic process with a power spectral density of the type

$$S_{j_h} = |H_j(\omega)|^2 S_h(\omega), \tag{15}$$

where $S_h(\omega)$ is the PSD of the GW background.

We can do the same consideration for the acceleration noise and write:

$$S_{j_g} = |G_j(\omega)|^2 S_g(\omega). \tag{16}$$

	RMS response to GW for ideal LISA	ASD of acceleration noise noise for ideal LISA	Effective h noise for ideal LISA
X	$\simeq 8.87\sqrt{2}\tau^3\omega^3$	$\frac{32\tau^2\omega\sqrt{S_g}}{c}$	$\simeq \frac{2.5\sqrt{S_g}}{c\tau\omega^2}$
T	$\simeq 0.146\sqrt{2}\tau^6\omega^6$	$\frac{8\sqrt{2}\tau^4\omega^3\sqrt{S_g}}{c\sqrt{3}}$	$\simeq \frac{32\sqrt{S_g}}{c\tau^2\omega^3}$
ζ	$\simeq 0.0547\sqrt{2}\tau^4\omega^4$	$\frac{\sqrt{6}\tau^2\omega\sqrt{S_g}}{c}$	$\simeq \frac{32\sqrt{S_g}}{c\tau^2\omega^3}$

TABLE VIII. Effective h noise for equal-constant LISA armlength in case of averaging the square of the response for 1000 GW sources over the celestial sphere for the null combinations ζ and T vs. Michelson X.

We can then compute the effective h noise as

$$S_{j_{g/h}} = \frac{S_{j_g}}{|H_j(\omega)|^2}, \tag{17}$$

i.e., by dividing the PSD of the acceleration noise by the transfer function of the stochastic GW background for different TDI combinations.

We analyse here two cases. In the first we consider a perfect LISA triangle and 1000 GW sources coming from multiple directions, in the second a non perfectly equilateral triangle and the GW sources coming orthogonal with respect to the LISA detector.

Thus, for the first case the transfer function reads

$$S_{j_h} = \sum_{i}^{N_s} |H_j^i(\omega)|^2 S_{h_i}(\omega), \tag{18}$$

with N_s as the number of sources. Here, each $S_{h_i}(\omega)$ is the PSD of the RMS of the $h_\times$ and h_+ polarizations of the GW. In practice, we consider both $h_\times$ and h_+ to be white noise processes with an ASD of $\frac{1}{\sqrt{Hz}}$ to compute the transfer functions $|H_j^i(\omega)|^2$. In TABLE VIII we report this effective h noise alongside the ASD of the acceleration noise and the RMS response to a wave for an ideal LISA where we averaged over the celestial sphere for T, ζ and TDI X.

In the second case, we consider only a single stochastic source orthogonal to the LISA plane, and take the inequality of the armlengths into account. We again compute the response to the single stochastic source, the acceleration noise as well as the effective h noise,

	Response to a GW coming orthogonal to the plane for slant LISA	ASD of acceleration noise for slant LISA	Effective h noise for slant LISA
X	$8\sqrt{6}\tau^3\omega^3$	$\frac{32\tau^2\omega\sqrt{S_g}}{c}$	$\frac{2\sqrt{2}\sqrt{S_g}}{\sqrt{3}c\tau\omega^2}$
T	$12\sqrt{3}\tau^3\omega^3\delta_r$	$\frac{8\tau^2\omega\sqrt{S_g}\sqrt{18\delta_r^2+\frac{2\tau^4\omega^4}{3}}}{c}$	$\frac{2\sqrt{S_g}\sqrt{\frac{2\tau^4\omega^4}{3}+18\delta_r^2}}{3\sqrt{3}c\tau\omega^2\delta_r}$
ζ	$\frac{3}{2}\sqrt{3}\tau^3\omega^3\delta_r$	$\frac{\sqrt{6}\tau^2\omega\sqrt{S_g}}{c}$	$\frac{2\sqrt{2}\sqrt{S_g}}{3c\tau\omega^2\delta_r}$

TABLE IX. Effective h noise for non equal-constant LISA arm-length in the case of a GW coming orthogonal to the LISA plane, for the null-combinations ζ and T vs. the Michelson X. Notice that the acceleration noise terms for ζ and X are not affected by the inequality of the arms and are equal to those given in Table VIII.

for T, ζ and TDI X. The result is summarized in TABLE IX.

Considering a realistic value of $\delta_r \approx 0.009$ [19], the effective h noise of T is much smaller than that of ζ. Thus, at least at low frequencies, ζ is a better noise monitor for the case of an orthogonal GW signal and unequal arm-length LISA, since it suppresses GW signals more effectively than T.

We plot the in Fig. 5 the effective h noise for T, ζ and TDI X, as given in TABLE VIII and TABLE IX.

We see that in case of a very simplistic GW background and ideal LISA, ζ and T show to have the same sensitivity while X is much more sensitive to GW. Thus, we can state that under these assumptions in the case of equal arms both T and ζ see the same signals and are better noise monitor than X. Conversely, considering the case of LISA with unequal arm-length and with a GW source orthogonal to the plane, for frequencies lower than around 10^{-2} Hz, ζ is less sensitive to GW than T, which means that we will be able to observe our instrumental noise in the presence of larger signals. Indeed, at least at low frequencies, T shows to have the same sensitivity as TDI X, which is well known to be sensitive to GW signals. This is different for higher frequencies where T flattens whereas ζ shows to decrease following a constant slope, thus T might be a better noise monitor than ζ in this frequency region. However, note that it is more difficult to estimate the exact combination of the acceleration noise of the six test-masses measured by T compared to the very simple rotational signal measured by ζ, especially in the case of unequal arms.

For completeness, since with this paper we want to suggest which are the TDI channels to use for estimating the instrumental noise, in Fig. 6 we report a comparison between sim-
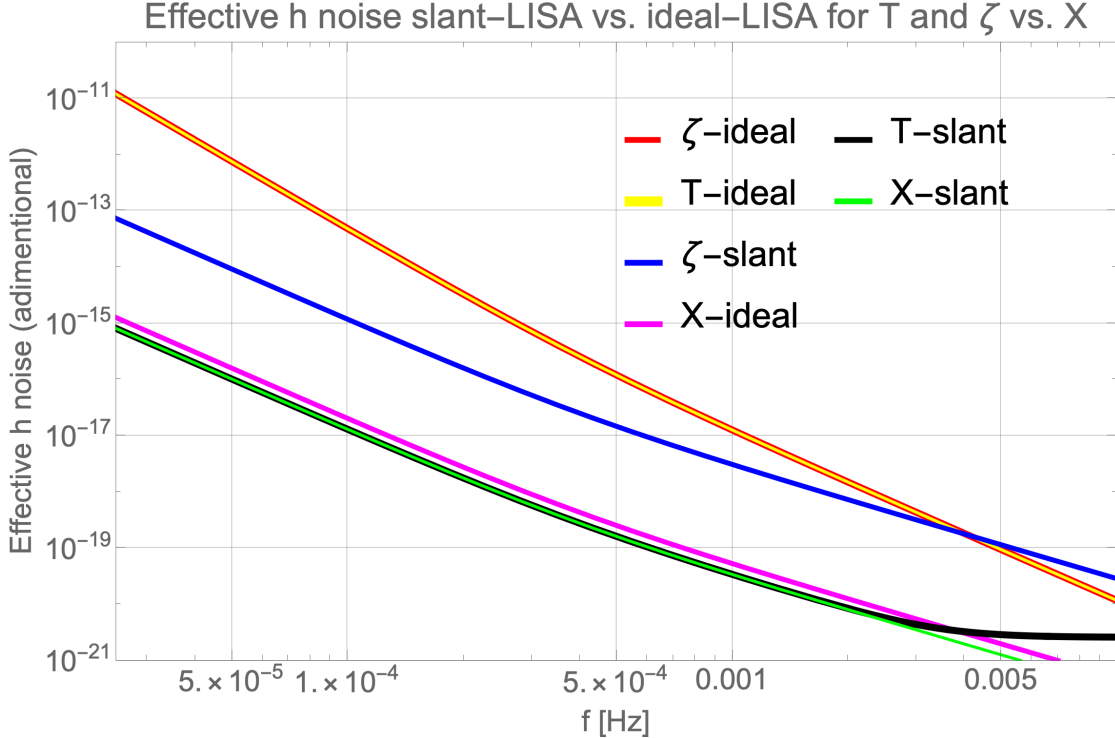
FIG. 5. The effective h noise for ζ and T for both slant and ideal LISA. The graph is made considering a stochastic GW-type signal with RMS of $\sqrt{2}$ and acceleration noise with the six test masses having the same ASD equal to $S_g^{1/2} = 2.4 \times 10^{-15} \sqrt{1 + \left(\frac{0.4 \times 10^{-3}}{f}\right)^2}$.

ulations using realistic LISA orbits, and the analytical models with ideal perfect equilateral LISA constellation, for the residual TM acceleration noise for T, ζ and X. The instrument simulation is performed using LISANode [5], while the TDI combinations are computed using the python tool pyTDI [20]. The power spectral density has been estimated using the Welch method, using the *Nutall4* window function.

We notice that for T, the approximated analytical model that considers equal constant arm-lengths does not accurately describe the TM acceleration noise at low frequencies. This is expected, and our model accounting for inequalities in the arms given in TABLE IX explains the observed noise level well. I.e., T no longer measures the simple signal proportional to ΔG_4 (at low frequency) when considering more realistic orbits.
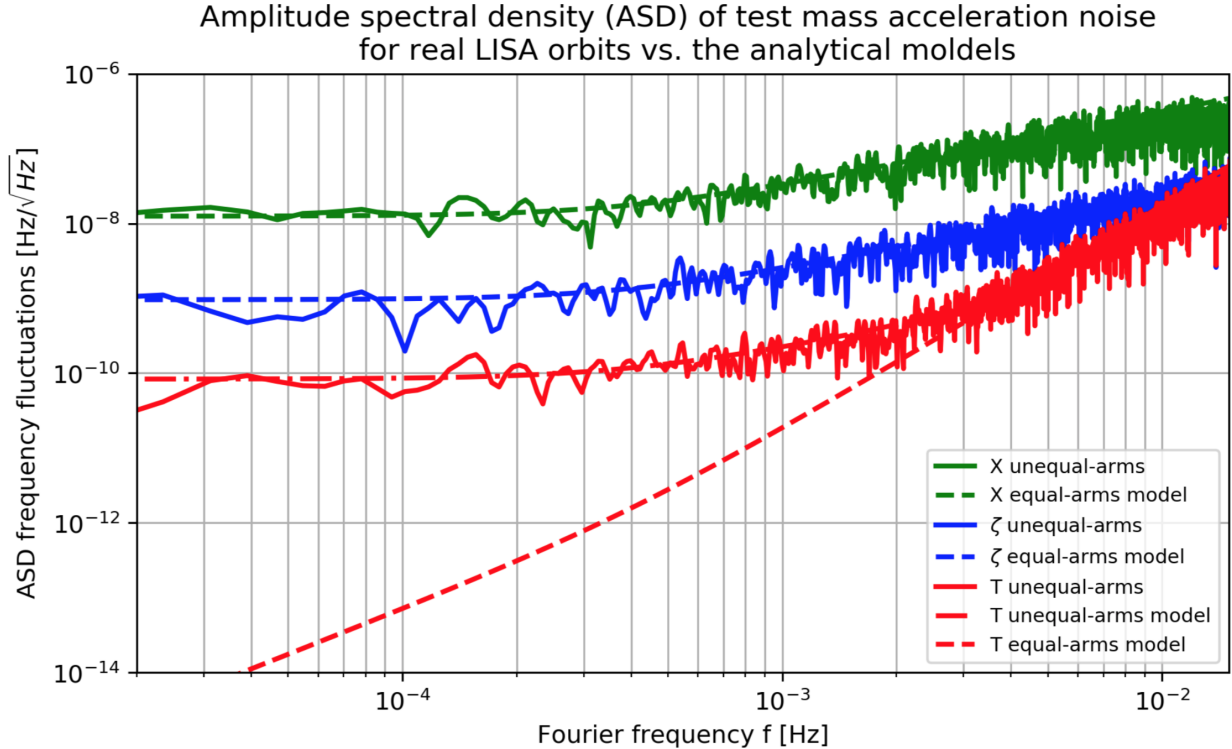
FIG. 6. Amplitude spectral density of the test-mass acceleration noise for the null-channel T and the Fully-Symmetric-Sagnac vs. TDI X compared with the respective analytical model. The simulations are performed considering ESA orbits

5.   DISCUSSION AND CONCLUSION

If we go up to 16-link combinations, and if we do not value the additional information that came from doing a time derivative, or a time finite difference, all information regarding the acceleration noise measurable using null combinations is already contained in the fully symmetric Sagnac combination ζ. Thus we only need one combination to measure the properties of this noise and to characterise the instrument.

With the combination ζ we measure a second derivative of a particular linear combination of the test masses that resembles the rigid rotation of the constellation. Other TDI combinations insensitive to a GW signal measure combinations of higher order derivatives of the same signal.

Indeed, T in the idealised condition of a perfect triangle measures the fourth derivative. We show that in the case of a stationary, isotropic and very simplified GW stochastic background, and LISA with equal and constant arms, ζ suppresses GW equally well as the combination T.

20

Regardless T behaves differently from ζ, at least from the theoretical calculation presented here, in the case of a constellation with un-equal but constant arms, and a simplified GW stochastic signal coming orthogonal to the LISA plane. Indeed there are other terms of the TM noise that contribute and overcome the rotational signal. In addition, we showed that ζ is significantly less sensitive to GW then T at low frequency when considering unequal arm-length, making it a better candidate to measure instrumental noise.

Ideally, we would like to monitor the instrumental noise independently from the GW background. Unfortunately, the fact that all null combinations only measure one type of acceleration signal which is, to zeroth order, orthogonal to the one that affects TDI X (which is the combination advertised in data analysis for detecting GW signal) severely limits the possible noise correlation analyses between the X channel and the null channels.

In conclusion, we found that these null-channels are useful as LISA noise monitors. They show to be sensitive to a signal which resembles the rigid rotation of the constellation. Note that all of these null channels need all 3 LISA arms to be constructed, such that in case we loose one arm of the constellation we also loose our ability to construct null channels. We are then left with just combinations such as the Michelson interferometer, which are strongly sensitive to GW signals. We plan to translate the results presented here into a more realistic LISA noise scenario and suggest the proper noise measurement approach for the LISA mission.

6.   ACKNOWLEGEMENT

Appendix A: Single value decomposition to retrieve the acceleration noise signals

Considering the single value decomposition, in our specific case we have U_{ik} as a 92×92 matrix, W_{kl} which is a 92×54 matrix, which has only the 7 uppermost diagonal elements different from zero, and V_{lj} which is a 54×54 matrix. Therefore the singular value decomposition of the acceleration matrix of coefficients δ_{ij} is

$$\delta_{ij} = \sum_{k=1}^{N} \sum_{l=1}^{54} U_{ik} W_{kl} V_{lj}^{T}, \tag{A1}$$

with $N = 92$ the number of null combinations. If we then multiply Eq. (A1) by the inverse of U_{ik} we get a 92×54 matrix that has only the first 7 lines different from zero:

$$\sum_{i=1}^{N} U_{mi}^{-1} \delta_{ij} = \sum_{l=1}^{54} W_{ml} V_{lj}^{T}. \tag{A2}$$

This allows us to redefine

$$\tilde{\psi}_m = \sum_{i=1}^{N} \sum_{k=1}^{102} U_{mi}^{-1} c_{ik} \psi_k(t), \tag{A3}$$

for which only the first 7 entries are non-zero. $\psi_k(t)$ are the 102 TDIs that are a subset of the 210 channels, see Supplemental Material at [URL] for the full list, and c_{ik} are the coefficients of one possible linear combination of the 210 TDIs null to GW (see Eq. (4)).

This reduced set of null-channels give us a better understanding of the reason why the rank R is 7. Indeed, in Eq. (A3) are different from zero only the signals for $m \leq R$, as for any value of m the GW part of the signal is zero. Besides for $m > R$ also the TM acceleration signal is zero.

REFERENCES

[1] M. Muratore, D. Vetrugno, and S. Vitale, Classical and Quantum Gravity **37**, 185019 (2020).

[2] M. Muratore, *Time delay interferometry for LISA science and instrument characterization*, Ph.D. thesis, University of Trento (2021).

[3] O. Hartwig, *Instrumental modelling and noise reduction algorithms for the laser interferometer space antenna*, Ph.D. thesis, Leibniz Universität Hannover (2021).

[4] These combinations could be reduce to a subset of 28 of 16-links, 3 of 14-links and 3 of 14-links, if one considers as equal combinations that differ for the any permutations of satellites and time reversal symmetry. We consider these 34 combinations as the core subset of the 210 total combinations.

[5] J.-B. Bayle, *Simulation and Data Analysis for LISA: Instrumental Modeling, Time-Delay Interferometry, Noise-Reduction Performance Study, and Discrimination of Transient Gravitational Signals*, Ph.D. thesis, Université de Paris (2019).

[6] M. Tinto and S. Dhurandhar, Living Reviews in Relativity **24** (2021), 10.1007/s41114-020-00029-6.

[7] M. R. Adams and N. J. Cornish, Phys. Rev. D **89**, 022001 (2014).

[8] The acceleration noise is any local disturbance acting on the test-mass (TM) that depends on many physical effects which locally perturbs the LISA TM geodesic motion inside the Gravitational Reference Sensor. It can be measured as an acceleration of the TM with respect to a local inertial reference frame, and has been demonstrated by LISA Pathfinder to be within the mission requirements [21].

[9] M. Maggiore, *Gravitational Waves: Volume 1: Theory and Experiments*, Gravitational Waves (OUP Oxford, 2008).

[10] Note that a GW is a non-local effect and can't be expressed as the combination of two local effects acting separately on the two satellites.

[11] Note that in defining these coefficients, we fix the time at which each TDI combination is measured. A more conclusive search would allow time shifts between the different combinations, which might allow us to find further null channels. We will explore how the TDI combinations relate to each other under timeshifts in a follow-up article [12], where we will demonstrate that such time shifts do not help in recovering additional information.

[12] O. Hartwig and M. Muratore, "Time delay interferometry generators for lisa secondary noises," (2021).

[13] To exclude the possibility that it might be due to our approximation of considering equal and constant arm-lengths, we also checked their behaviour for a non-equal arm-length constellation and get the same result. Therefore we conclude that these combinations are mathematical artefacts and do not seem to have a practical purpose.

[14] This is valid as LISA is a perfect triangle.

[15] In detail, we have

$$
\begin{aligned}
\Delta G_0 &= G_0 \\
\Delta G_1 &= G_0 - G_1 \\
\Delta G_2 &= G_0 - 2G_1 + G_2 \\
\Delta G_3 &= G_0 - 3G_1 + 3G_2 - G_3 \\
\Delta G_4 &= G_0 - 4G_1 + 6G_2 - 4G_3 + G_4 \\
\Delta G_5 &= G_0 - 5G_1 + 10G_2 - 10G_3 + 5G_4 - G_5 \\
\Delta G_6 &= G_0 - 6G_1 + 15G_2 - 20G_3 + 15G_4 - 6G_5 + G_6 \\
\Delta G_7 &= G_0 - 7G_1 + 21G_2 - 35G_3 + 35G_4 - 21G_5 + 7G_6 - G_7 \\
\Delta G_8 &= G_0 - 8G_1 + 28G_2 - 56G_3 + 70G_4 - 56G_5 + 28G_6 - 8G_7 + G_8
\end{aligned}
$$

.

[16] It might also help for an actual implementation of these combinations, since each of these null-channels is built out of combinations which belong to the same topology. Indeed, for the combinations T, we had just to sum the X,Y,Z without applying any additional delays. This means we can construct them without considering relative timeshifts between combinations of different topology.

[17] A. Nussbaum, American Journal of Physics **36**, 529 (1968), https://doi.org/10.1119/1.1974965.

[18] What we call here effective h noise is also often referred to as strain sensitivity, given by renormalizing the instrument noise PSD by the gravitational wave transfer function of the instrument, see e.g. [22].

[19] We obtained the estimation of the δ_r inverting the 13 for L_{12}, L_{23} and L_{32}, and using the ESA orbits used in LISANode, cf. [5].

[20] The original codebase for pyTDI was developed by M. Staab and J.-B. Bayle, and it is now

being developed by multiple contributors inside the LISA Consortium.

[21] E. Castelli, *LISA Pathfinder noise performance results: disturbances in the sub-mHz frequency band and projection to LISA*, Ph.D. thesis, Trento U. (2020).

[22] S. L. Larson, W. A. Hiscock, and R. W. Hellings, Physical Review D **62** (2000), 10.1103/physrevd.62.062001.